J. Wind Eng. Ind. Aerodyn. 133 (2014) 242–249

Contents lists available at ScienceDirect

Journal of Wind Engineering and Industrial Aerodynamics

journal homepage: www.elsevier.com/locate/jweia

Hurricane wind hazard assessment for a rapidly warming climate scenario

Lauren Mudd *, Yue Wang, Christopher Letchford, David Rosowsky [1]

Rensselaer Polytechnic Institute, 110 8th St. Troy, NY, USA

ARTICLE INFO

Keywords:
Hurricane wind hazard
Climate change
Sea surface temperature
Stochastic hurricane models
Monte Carlo simulation

ABSTRACT

Although there is still much debate as to the causes, it is generally accepted in the scientific community that the climate is changing. The IPCC (2007) Fourth Assessment Report states that warming of the climate system is unequivocal, and that this warming has likely influenced observed changes in many physical systems at the global scale. In order to meet target safety and performances levels when designing structures and infrastructure systems in the future, it is essential that current design codes and standards adapt to reflect global climate change. With the trend toward performance-based engineering, for US coastal regions, along the Atlantic Ocean and Gulf of Mexico, this means a quantitative assessment of climate change impact on hurricane hazard performance levels is needed.

This study couples a projected climate change scenario with state-of-the-art probabilistic event-based simulation procedures to assess the hurricane wind hazard under a worst-case climate change scenario. The hurricane wind hazard is defined herein using the hurricane intensity (maximum wind speed) and hurricane size (radius to maximum wind speed). Through Monte Carlo simulation, 10,000 years of hurricane events, under the current (2012) and future (2100) climate conditions, were generated. The hurricane intensity distribution and the joint distribution of hurricane intensity and size, under current and future climate scenarios, were then compared.

1. Introduction

Hurricanes cause extreme weather and severe damage along impact zones, such as the US east coast, putting major urban population centers at risk. In 2012, US landfalling hurricanes accounted for 143 of the 284 US fatalities caused by natural disasters, and over $52 billion in losses (Rosenthal et al., 2013). The severity of hurricane hazards has led to many studies seeking to improve forecasting, warning and evacuation. However, as meso-scale meteorological events hurricanes are affected by climate change (Emanuel, 1987, 2008; Bender et al., 2010), the impact of which has received little attention to date. In order to continue to ensure the safety of our built world in the future, current design codes and standards must be adapted to account for future climate change impacts on hurricane hazards (wind, surge, flood). The study performed herein makes use of similar probabilistic simulation procedures used in the development of wind speed maps contained in the US design standard ASCE 7 from the years 1993 (ASCE, 1993) through 2010 (ASCE, 2010), and can serve as a basis for updating coastal design wind speeds for future editions.

There have been some initial studies to examine the effect of climate change scenarios on wind, storm surge and flooding in recent years. Nishijima et al. (2012) conducted an impact assessment of climate change on the northwest Pacific typhoon wind risk, focusing on potential damages to residential buildings in Japan. In their work, typhoons were simulated using the Atmospheric General Circulation Model (AGCM) under the 2005 and future climate scenarios. Similar procedures were adopted herein; however, the atmospheric model, the projected scenarios and hurricane models are different, as explained in the following sections. Irish. (2008) examined the influence of climate change on hurricane flooding for Corpus Christi, TX and Lin et al. (2012) investigated the influence of climate change on hurricane induced storm surge for New York, NY. However, the hurricane models used in the two previous studies were deterministic.

The availability of the historical Hurricane Database (Hurdat, 2013) maintained by the National Hurricane Center (NHC) has enabled event-based simulation procedures (Vickery et al., 2000a,2000b) to be developed in the public sector. In Mudd et al. (2014), state-of-the-art hurricane prediction models were used to

* Corresponding author. Tel.: +1 5028363942.
E-mail addresses: muddl@rpi.edu (L. Mudd), wangy20@rpi.edu (Y. Wang), letchc@rpi.edu (C. Letchford), david.rosowsky@uvm.edu, rosowd@rpi.edu (D. Rosowsky).
[1] Present Address: Provost and Senior Vice President, Office of the Provost, University of Vermont, 348 Waterman Building, 85 S Prospect St., Burlington, VT, USA.

http://dx.doi.org/10.1016/j.jweia.2014.07.005
0167-6105/

simulate hurricanes in the year 2100 under IPCC climate change scenario RCP 8.5. A framework developed by Lee and Rosowsky (2007) was then implemented to develop a hurricane wind speed database for the Northeast US coast, including the states of Maryland, Delaware, New Jersey, Pennsylvania, New York, Connecticut, Rhode Island, Massachusetts, Vermont, New Hampshire and Maine, under both the 2005 and future climate states. Note that although Vermont and Pennsylvania are not coastal states, they have been affected by hurricanes in the past (e.g., Irene in 2011) and were considered as part of the hurricane-prone US Northeast. Key components of the simulation framework used in Mudd et al. (2014) were the gradient wind-field model (Georgiou, 1985) and the tracking and central pressure models (Vickery et al., 2000a, 2000b). The post-landfall decay model proposed by Vickery and Twisdale (1995) was used with site specific decay constants determined through statistical analyses of historical data. Finally, trends in hurricane genesis frequency and hurricane track were also explored.

The assessment presented herein represents an update to the analysis performed in Mudd et al. (2014). Since the development of the hurricane simulation techniques (Vickery et al., 2000a, 2000b) used in Mudd et al. (2014), significant improvements have been made (Vickery et al. 2009). These improvements consist of an updated statistical model for the determination of the Holland pressure profile parameter and the radius to maximum winds (Vickery and Wadhera, 2008), and a new model for hurricane decay after landfall (Vickery, 2005). In addition, several major hurricane events have occurred since 2005, which was used as the current scenario in Mudd et al. (2014). The study presented herein makes use of all available historical hurricane data to extend the current scenario to the year 2012. In addition, the most current historical hurricane database (HURDAT, 2013) incorporates findings of several re-analysis projects (Landsea et al., 2004a, 2004b, 2008, 2012; Hagen et al., 2012) to correct errors and biases that have previously appeared in the historical data. While storm surge and flooding due to hurricanes also cause damage, only the direct hurricane wind hazard (maximum wind speed and storm size) is considered herein. The Northeast US coast was selected as the sample study region; however, the framework can be applied in other hurricane affected regions as well. Details of the projected future climate change scenarios and the probabilistic hurricane simulation models are described in the following sections.

2. Projected future climate change scenarios

Representative Concentration Pathway (RCP) scenarios have been developed recently for climate change projections for the IPCC Fifth Assessment Report (to be published October 2014) and future editions. A discussion of the RCP scenarios can be found in Mudd et al. (2014). In this study, only the worst-case projected future climate change scenario, RCP 8.5, was considered. RCP 8.5 is a "high forcing" scenario with 8.5 W/m^2 total radiative forcing in the year 2100. Comparatively, the 2005 radiative forcing level, according to IPCC Fourth Assessment Report (IPCC, 2007), is 1.6 W/m^2. The radiative forcing estimates are primarily based on the forcing of greenhouse gases. All climate change scenarios from January 2005 to December 2100, based on the RCP 8.5 pathway projection, were simulated using the Community Earth System Model (CESM, 2012). CESM (2012) is a fully coupled, global climate model that provides state-of-the-art computer simulations of the Earth's past, present, and future climate states. As the driving parameter of most hurricane models, the monthly average sea surface temperature (SST) values were then extracted from the CESM (2012) simulation for use in the hurricane simulation procedures described in the following section. The SST values were originally stored on a displaced-pole grid and were transformed to lie on the regular rectangular $1^\circ \times 1^\circ$ grid. The difference between the current and future SST in August, the most active hurricane month, is shown in Fig. 1. As shown in Fig. 1, the largest SST increases are along the Northeast US/Canadian coast.

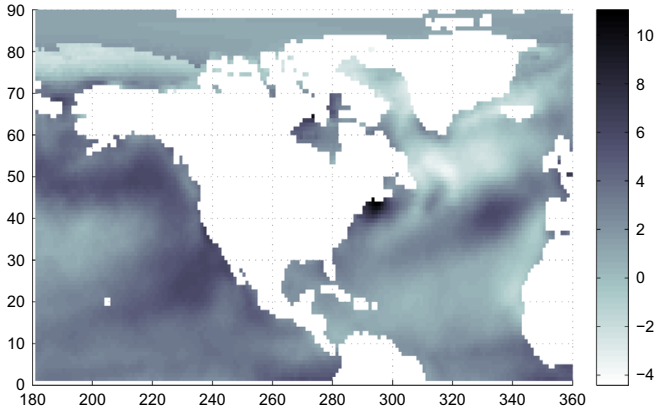

Fig. 1. Projected SST change (°C) under climate change scenario RCP 8.5 from August 2012 to August 2100.

3. Probabilistic hurricane modeling and simulation procedures

3.1. Hurricane genesis model

Simulated hurricanes are generated according to a Poisson arrival process. Considering all storms generated in the Atlantic basin and assuming a constant annual hurricane occurrence rate with time, the annual hurricane occurrence rate, λ, for the year 2012 was found to be 8.4 based upon work performed by Lee and Rosowsky (2007). Also considering all storms generated in the Atlantic basin, Mudd et al. (2014) used a least-squares regression to fit a linearly increasing trend to the annual hurricane occurrence rate and found λ for the year 2100 to be 13.9. However, when considering only historical hurricanes that made landfall in the US, no linearly increasing trend in annual hurricane occurrence rates is seen (Mudd et al., 2014), and λ is found to be approximately 2.9 hurricanes per year. The historical data and fitted trends are shown in Fig. 2 for all hurricanes occurring in the Atlantic basin and for only hurricanes making landfall in the US.

Several recent studies (Mann and Emanuel, 2006; Holland and Webster, 2007; Mann et al., 2007; Knutson et al., 2008; Landsea et al., 2010; Vecchi and Knutson, 2008) have examined the completeness of the HURDAT database and its validity in determining the frequency of occurrence of historical hurricane events. Due to the high variability of frequency of storms from year to year, as well as physical limitations of past observing and reporting capabilities, no consensus has been reached on the subject. However, in regards to the accuracy of the record of US landfalling hurricanes, there is little debate. Using population data from US census reports and other historical analyses, Landsea et al. (2004a) provided dates for when landfalling hurricane records in specified regions of the US could be deemed accurate. For every geographical region considered, they concluded that the records were accurate after 1900, and that the records along the US Northeast coast may be accurate as far back as 1660. In order to remove a source of uncertainty from the simulations performed herein, this study utilizes an annual hurricane genesis frequency based only upon historical events that made landfall in the US. In addition, limiting the number of historical hurricanes to only those that made landfall in the US results in a lower annual hurricane genesis frequency to be used during simulation (since the number of hurricanes generated that hit the US annually is much less than the total number of hurricanes generated

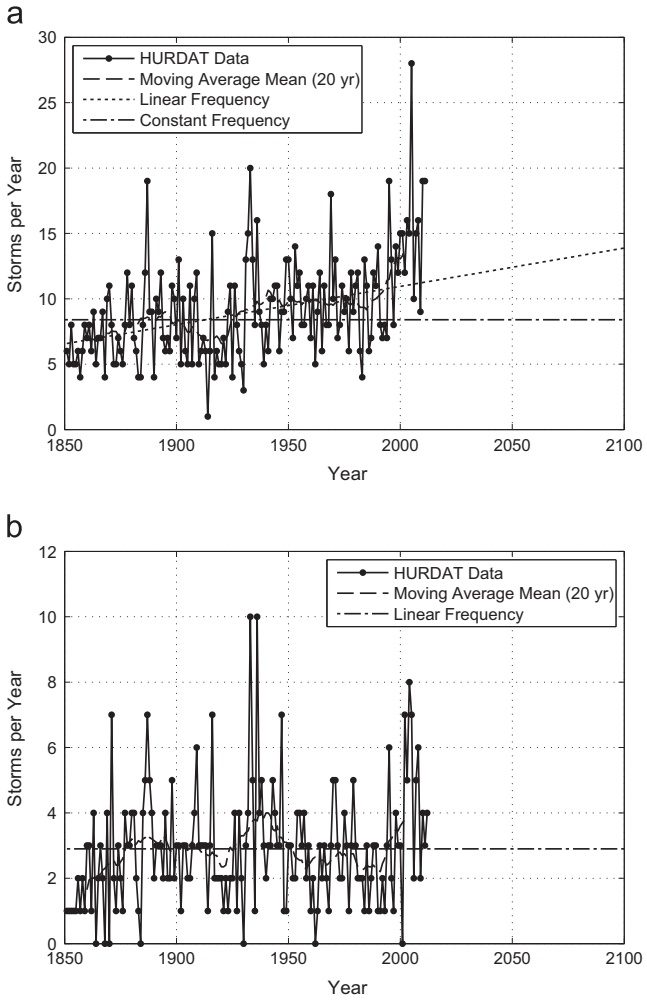

Fig. 2. Frequency of (a) all hurricanes generated in the Atlantic basin and (b) only hurricanes that made landfall in the US.

in the Atlantic basin annually.) In generating fewer events during simulation, the required computation time is significantly reduced.

3.2. Georgiou's gradient wind field model

Using information obtained by aircraft reconnaissance observations, the hurricane gradient wind speed can be defined. Aircraft typically record wind speeds at an elevation of 3000 m, which is higher than gradient-level wind speeds, which occur 500–2000 m above the surface. However, it has been shown, by Powell (1990) and Sparks and Huang (1999), that wind speeds measured between 2000 and 3000 m show little variation. Consistent with historical data obtained by aircraft reconnaissance and as shown in a number of other studies (e.g., Rosowsky et al., 1999), well-formed hurricane gradient wind fields can be represented as a vortex with translational movement. Therefore, the gradient wind speed, V_g, can be decomposed into a rotational component, V_R, and a translational component, V_T.

Since the rotational wind speed is assumed to be symmetrical about the hurricane eye in this study, the rotational component, V_R, can be described as a function of distance from the hurricane eye. The gradient rotational wind speed vortex can then be determined using this rotational wind speed component. Georgiou's model (Georgiou, 1985) describes the rotational vortex shape through Eq. (1).

$$V_g^2(r,\alpha) = \frac{r}{\rho}\frac{\partial P}{\partial r} + V_g(r,\alpha)\,(V_T \sin\alpha - f\,r) \tag{1}$$

where V_g=gradient wind speed, r=distance from hurricane eye, α=angle from hurricane heading direction (counter-clockwise +), ρ=air density, V_T=translational wind speed, f=coriolis parameter and P=surface air pressure. Information needed to statistically characterize these parameters (central pressure, storm track and translational speed) can be obtained from the HURDAT database. The surface air pressure $P(r)$ at a distance r from the hurricane eye is given by Eq. (2) (Vickery et al., 2000b):

$$P(r) = P_c + \Delta P \exp\left[-\left(\frac{R_{max}}{r}\right)^B\right] \tag{2}$$

where P_c=air pressure at the hurricane eye, ΔP=the central pressure deficit (mb)=1013-P_c (mb), R_{max}=radius of maximum winds, and B=pressure profile parameter. As an update to Mudd et al. (2014), this study uses models developed by Vickery and Wadhera (2008) to calculate R_{max} and B as functions of the hurricane eye latitude, ψ, central pressure deficit, ΔP, and region. Two models to calculate R_{max} were recommended, one for hurricanes located in the Atlantic Ocean and one for hurricanes located in the Gulf of Mexico. The best single equation estimates for R_{max} for the Atlantic Ocean and the Gulf of Mexico are given by Eqs. (3) and (4) respectively.

$$\ln(R_{max})_{Atlantic} = 3.015 - 6.291(10^{-5})\Delta P^2 + 0.0337\psi + \varepsilon_{Atlantic} \tag{3}$$

$$\ln(R_{max})_{Gulf} = 3.859 - 7.700(10^{-5})\Delta P^2 + \varepsilon_{Gulf} \tag{4}$$

where $\varepsilon_{Atlantic}$ and ε_{Gulf} are modeled as Normal (0, 0.441) and Normal (0, 0.390) respectively. The Atlantic Ocean estimate is used for all hurricane steps east of 80°W and the Gulf of Mexico estimate is used for all hurricane steps west of 80°W and north of 18°N. Eqs. (3) and (4) are combined through Eq. (5) to yield one statistical model to determine R_{max} at each step of every simulated storm.

$$R_{max} = a_1(R_{max})_{Atlantic} + (1-a_1)(R_{max})_{Gulf} \tag{5}$$

where a_1 is given by Eq. (6).

$$a_1 = \sum \Delta P_{Atlantic} / \sum(\Delta P_{Atlantic} + \Delta P_{Gulf}) \tag{6}$$

Prior to landfall, the Holland pressure profile parameter, B, is given by Eq. (7).

$$B = 1.7642 - 1.2098\sqrt{A} \tag{7}$$

where A is given by Eq. (8):

$$A = fR_{max} \Big/ \sqrt{2R_d(T_s - 273)\ln(1 + \Delta P/(P_c e))} \tag{8}$$

where R_d=gas constant for dry air, T_s=sea surface temperature (°K), and e=base of natural logarithms. After making landfall, B is modeled by Eq. (9).

$$B = B_0 \exp(a_2 t) \tag{9}$$

where B_0=value of B at landfall, and a_2 is given by Eq. (10).

$$a_2 = 0.0291 - 0.0429B_0, \quad a_2 \le -0.005 \tag{10}$$

After the surface air pressure is calculated using Eqs. (2) (through 10), the gradient surface air pressure, $\partial P/\partial r$, can be calculated and substituted into Eq. (1). The gradient wind speed, V_g, then takes the form of Eq. (11) (Vickery et al., 2000b).

$$V_g = \frac{1}{2}(cs\sin\alpha - fr) + \sqrt{\frac{1}{4}(cs\sin\alpha - fr)^2 + \frac{B\Delta P}{\rho}\left(\frac{R_{max}}{r}\right)^2 \exp\left[-\left(\frac{R_{max}}{r}\right)^2\right]} \tag{11}$$

3.3. Vickery's empirical storm tracking and central pressure model

An empirical tracking model was proposed by Vickery et al. (2000b) to describe the hurricane translational wind speed and heading angle. In this study, the entire Atlantic basin was divided into

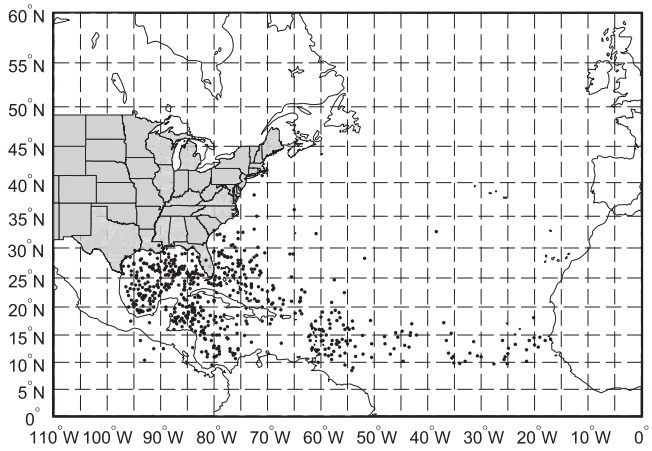

Fig. 3. Initial positions of US landfalling hurricanes in the HURDAT database and $5^\circ \times 5^\circ$ grid division for the Atlantic basin.

$5^\circ \times 5^\circ$ grid blocks, as shown in Fig. 3. Each grid block has its own grid-based parameters which are used to determine the translational wind speed and heading angle at next time-step by Eqs. (12) and (13) respectively.

$$\Delta \ln c = a_1 + a_2\psi + a_3\lambda + a_4 \ln c_i + a_5\theta_i + \varepsilon \tag{12}$$

$$\Delta\theta = b_1 + b_2\psi + b_3\lambda + b_4 c_i + b_5\theta_i + b_6\theta_{i-1} + \varepsilon \tag{13}$$

where c=translational velocity (translational wind speed), θ=heading angle, a_i (i=1,2,…5)=coefficient for translational velocity, b_i (i=1,2,…6)=coefficient for heading angle, ψ and λ=storm latitude and longitude, c_i=translational velocity at time-step i, θ_i=heading angle at time-step i, θ_{i-1}=heading angle at time-step i-1, and ε=random error term.

The HURDAT database contains data at 6-h intervals describing hurricane eye position, translational velocity, heading angle and central pressure for all hurricanes that have occurred in the Atlantic basin since 1851. Therefore, the coefficients a_i and b_i for each grid location can be determined through regression analysis of HURDAT data at each grid location. An analysis of the tracking parameters was performed in Mudd et al. (2014), in which two key conclusions were drawn. Firstly, it was concluded that there is a lack of evidence of climate-influenced changes in hurricane track characteristics. Secondly, through comparison of landfalling numbers and spatial behavior of hurricane tracks, it was shown that simulating hurricanes using tracking parameters based only upon historical US landfalling hurricanes (instead of all Atlantic basin hurricanes) sacrifices no agreement between simulated hurricane data and historical hurricane data.

Based upon these findings, tracking parameters in this study were determined from only those hurricanes that made landfall in the US from 1851 to 2012, and any impact of climate change on the parameters of Eqs. (12) and (13) was not considered in the simulation process (i.e. the Markov model used in the tracking model of this study was assumed to be stationary.) For those grid locations with little or no hurricane data, the coefficients were assigned the corresponding values from the nearest grid location.

The hurricane central pressure model suggested by Vickery et al. (2000b) was developed based on the relative intensity concept (Darling, 1991). The hurricane eye central pressure P_c can be expressed in terms of relative intensity I, and vice versa. The details of the relationship between hurricane eye central pressure and the relative intensity can be found in the appendix of Darling's paper (Darling, 1991). Of interest in the present study, the hurricane eye central pressure is described by Darling (1991) as a function of sea surface temperature as in Eq. (14).

$$\ln(I_{i+1}) = c_0 + c_1 \ln(I_i) + c_2 \ln(I_{i-1}) + c_3 \ln(I_{i-2}) + c_4 T_s + c_5 \Delta T_s + \varepsilon \tag{14}$$

where I_{i+1}=relative intensity at the time-step $i+1$; I_i, I_{i-1}, I_{i-2}=relative intensity at the time steps i, $i-1$ and $i-2$, c_i=the grid-based coefficient for relative intensity, T_s=sea surface temperature (K), ΔT_s=difference in sea surface temperatures at time-steps i and $i+1$ (K), and ε=random error term. Similar to the tracking model coefficients, the coefficient parameters c_i for each grid location can be determined by regression analysis, using the relative intensity values calculated from the HURDAT central pressure data at each grid location. For those grid locations with little or no hurricane data, the coefficients are assigned the corresponding value from the nearest grid location. After the hurricane makes landfall, the central pressure decays and the relative intensity approach is no longer applicable. For the current climate, the T_s (SST) value is taken as the 2012 SST data, and for the future climate scenario, the value is taken as the 2100 SST data. Thus, the effect of climate change on storm intensity and size is explicitly considered herein.

3.4. Decay model

Once a hurricane makes landfall, it is cut off from its energy source (the sea) and it reduces in strength. Increased surface friction overland also decreases the intensity, further contributing to the decay. Consequently, both the central pressure difference and the rotational wind speed decrease according to some decay model. The decay model (Vickery and Twisdale, 1995) used in this study takes the form of an exponential decay function as in Eq. (15).

$$\Delta P(t) = \Delta P_0 \exp(-a_3 t) \tag{15}$$

where $\Delta P(t)$=the central pressure deficit (mb) at time t after landfall, ΔP_0=the central pressure deficit (mb) at landfall, a_3=site-specific decay parameter (constant), and t=time after landfall.

In Mudd et al. (2014) the site-specific decay parameter a_3 was only a function of the central pressure deficit at landfall. Vickery (2005) found the site-specific decay parameter a_3 (in some regions) is more accurately modeled as a function of not only central pressure deficit at landfall, but also translational velocity c and radius to maximum winds R_{max}. This study uses the functions of a_3 as determined by Vickery (2005), which are given by Eqs. (16) (through 19).

$$\text{Gulf Coast}: \quad a_3 = 0.0413 + 0.0018(\Delta P_0 c/R_{max})\varepsilon +, \quad \sigma_\varepsilon = 0.0169 \tag{16}$$

$$\text{Florida (East Coast)}: \quad a_3 = 0.0225 + 0.0017(\Delta P_0 c/R_{max}) + \varepsilon, \quad \sigma_\varepsilon = 0.0158 \tag{17}$$

$$\text{Mid-Atlantic Coast}: \quad a_3 = 0.0364 + 0.0016(\Delta P_0 c/R_{max}) + \varepsilon, \quad \sigma_\varepsilon = 0.0161 \tag{18}$$

$$\text{North Atlantic Coast}: \quad a_3 = 0.0034 + 0.0010\Delta P_0 + \varepsilon, \quad \sigma_\varepsilon = 0.0114 \tag{19}$$

where the error term is modeled as a Normal (0, σ_ε).

3.5. Gradient to surface wind speed conversion

While the hurricane is inland, the surface wind speed, at a standard reference height of 10 m above the ground, can be estimated using conversion factors applied to the wind speed at the gradient level, generally taken as between 500 and 2000 m

above the ground. Open terrain conditions are assumed when describing the surface wind speed at the standard reference height. The gradient-to-surface wind speed conversion factors assumed herein for both 10-min sustained wind speeds and 5-s gust wind speeds are taken from Lee and Rosowsky (2007).

3.6. Simulation procedures

Simulated hurricanes start in the Atlantic basin with parameters based directly on a randomly selected US landfalling hurricane contained in the HURDAT database (i.e. initial location, angle, translational speed, and central pressure). The locations of hurricane formation for each event in the HURDAT database are shown in Fig. 3. The hurricane then moves along a track defined by the tracking and central pressure models. The hurricane's position at each subsequent 6-hour interval can be determined by Eqs. (12) and (13) using the parameters derived from the information in the HURDAT database. Similarly, the next interval's central pressure (intensity and size) can be obtained using Eq. (14). Once the hurricane makes landfall, the central pressure decays according to Eq. (15). Finally the gradient wind speed can be obtained from Eq. (11) and converted to a surface wind speed using the gradient-to-surface wind speed conversion factors found in Lee and Rosowsky (2007). If the simulated hurricane produces a significant maximum 10-min surface wind speed (defined herein as 15 m/s or greater) at any geographical location in the US Northeast, this value is recorded in the wind speed time series for the zip code which encompasses it.

Following this procedure, 10,000 years of simulated hurricane events are generated for both the current and future climate scenarios, and the simulated hurricane wind speed records are developed for every zip code in the study region. Based on a framework developed by Wang and Rosowsky (2012), in which the hurricane wind speed and storm size are jointly characterized using the descriptors of maximum gradient wind speed V_{max} (at the eye-wall) and the radius to maximum wind speed R_{max}, the values of these two parameters associated with the 10-year, 20-year, 50-year, 100-year, 300-year, 700-year, and 1700-year mean recurrence intervals (MRI's) are calculated. The results can then be compared, e.g., 2012 vs. 2100, to assess the impacts of possible future climate change effects on the hurricane intensity and size.

Note that in the study region considered in this paper (the US Northeast coast), the extreme wind climate may not be characterized by hurricane wind speeds only. Extra-tropical storms and thunderstorms also are expected to influence the extreme wind climate. Therefore, the simulated hurricane wind speed records developed herein can only be used (by themselves) to characterize the wind hazard close to the coast where the extreme wind climate is dominated by tropical storms (hurricanes).

4. Results comparison and discussion

The joint histogram, estimates of the probability of exceedance, and MRI's of the simulated events can be determined using the key descriptors V_{max} and R_{max} of the closest 6-h interval to landfall, using a framework developed by Wang and Rosowsky (2012). The simulated hurricanes were assumed to occur with more or less equal probability along the length of coastline of the study area. This equi-probability assumption has been validated in the past for the study regions of Texas (Wang, 2010) and North Carolina, South Carolina, and Virginia (Lee and Rosowsky, 2007) by analyzing the landfalling positions of the historical hurricane events in those regions. In the US Northeast however, while the landfalling positions are generally spread equally along the coastline, the basis for this assumption is not as robust due to the limited number of historical events to sample from. The historical landfalling rate on the US Northeast coast is approximately 0.11 hurricanes per year. The simulated landfalling rate under the current climate scenario was approximately 0.12 hurricanes per year, which agrees well with the historical landfalling rate for the study region. Under the future climate scenario RCP 8.5, the simulated landfalling rate was found to be approximately 0.15 hurricanes per year for the study region. Furthermore, the increase in landfalling rate was not found to be uniform over all hurricane intensities. For weaker hurricanes ($\leq$ Category 3) the landfalling rate was found to be approximately 0.11 hurricanes per year for both the current and future climate scenarios. When considering intense hurricanes ($\geq$ Category 4) the landfalling rate increased from approximately 0.01 hurricanes per year in the current climate scenario to approximately 0.04 hurricanes per year in the future climate scenario. With a constant rate of genesis, this implies intense hurricanes are more likely to make landfall in the future climate scenario simulation. The increase in simulated landfall events is uniform over the study region, as shown in Fig. 4.

The joint histogram can be constructed using data pairs of V_{max} and R_{max} recorded at the time of landfall. The joint histogram for each scenario is shown in Fig. 5. The annual joint exceedance probability was obtained, using the joint histogram, by dividing the number data pairs of V_{max} and R_{max}, within a specified bin, by

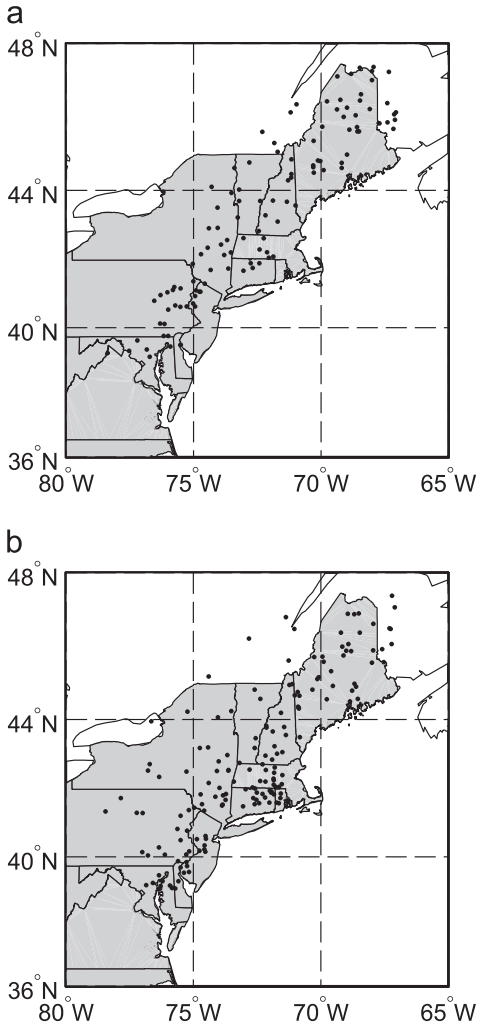

Fig. 4. Nearest 6-h location of hurricane eye to landfall in 1000 years of simulated events for the US Northeast coast under (a) the 2012 climate scenario and (b) the 2100 climate scenario.

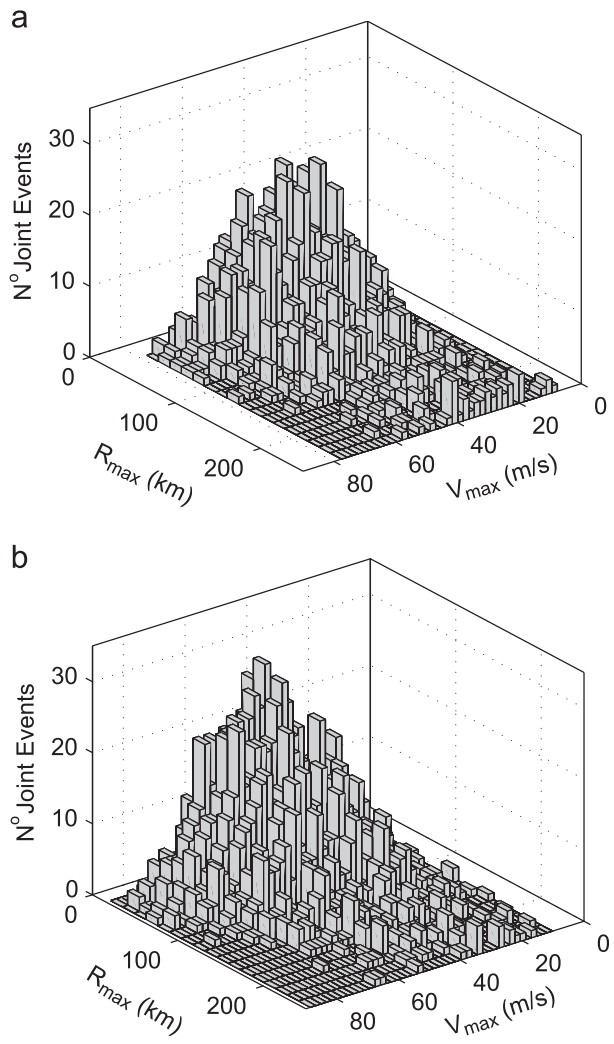

Fig. 5. Joint Histogram of V_{max} and R_{max} for (a) the 2012 climate scenario and (b) the 2100 climate scenario.

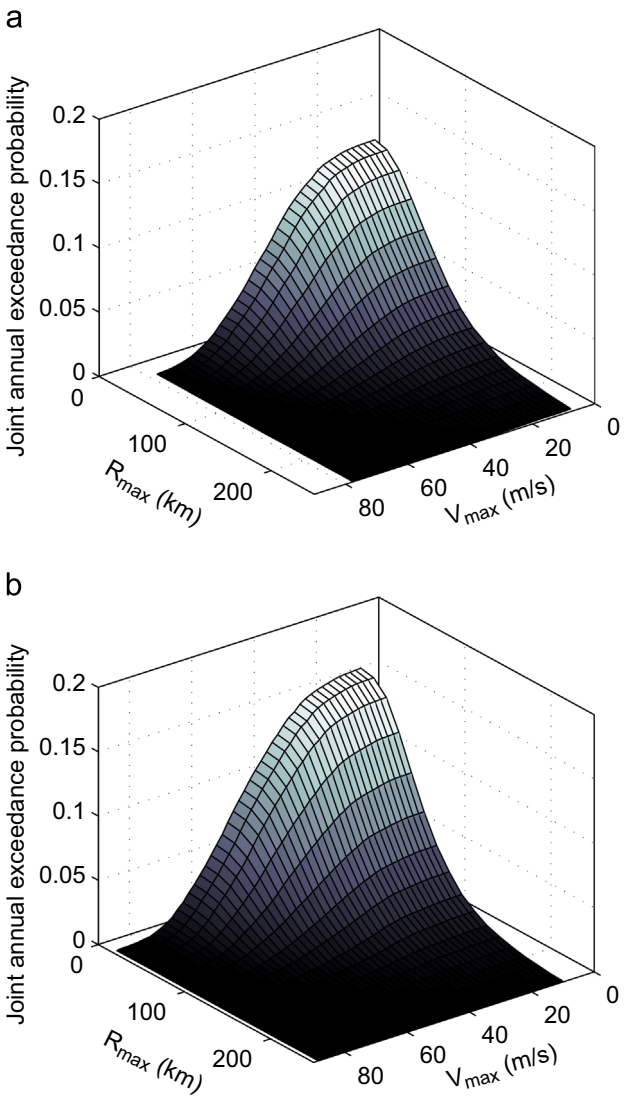

Fig. 6. Joint annual exceedance probability of V_{max} and R_{max} for (a) the 2012 climate scenario and (b) the 2100 climate scenario.

the total number of data pairs recorded in the simulation and multiplying by the annual hurricane occurrence rate, λ; see Fig. 6.

Once the annual joint exceedance probability of V_{max} and R_{max} was defined, the framework developed by Wang and Rosowsky (2012) was employed in which hazard levels with different annual exceedance probabilities can be described by equi-probability contours. The hazard level can also be described as an exceedance probability in N years (e.g. 2%/50 Years). The joint hazard level contours at the time of landfall corresponding to different MRI values, or annual exceedance probabilities, for each simulated future climate scenario, compared to those of the simulated 2012 climate scenario, are shown in Fig. 7. Fig. 7 shows that under future climate scenario RCP 8.5 in the year 2100, the maximum wind speeds associated with each hazard level are expected to increase, while the size of the hurricanes associated with each hazard level remains relatively constant.

For each location in the study region, the distribution of the N-year maximum wind speed under all considered climate scenarios can be fitted and used to examine any changes in hurricane wind climate at that location. As an example, we consider New York City. To determine the best-fit distribution for the 50-year maximum wind speed, four distribution types were considered: Lognormal, Extreme Type-I (ET-I), Extreme Type-II (ET-II), and Reverse Extreme Type-III (ET-III). The 50-year maximum wind speed best-fit distribution, under both the current and future

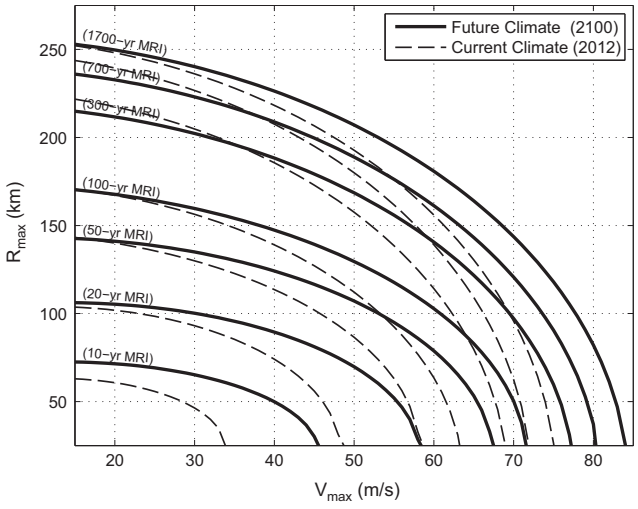

Fig. 7. Hazard level contours for the Northeast US coast under the 2012 climate scenario and the 2100 climate scenario.

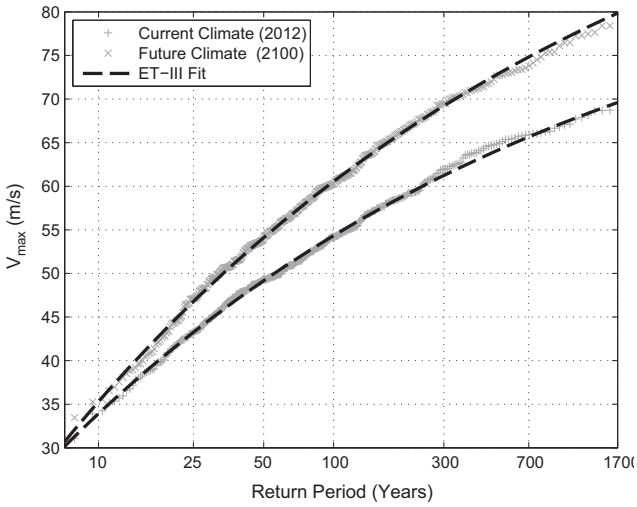

Fig. 8. 50-yr maximum wind speed distribution for New York City under the 2012 climate scenario and the 2100 climate scenario.

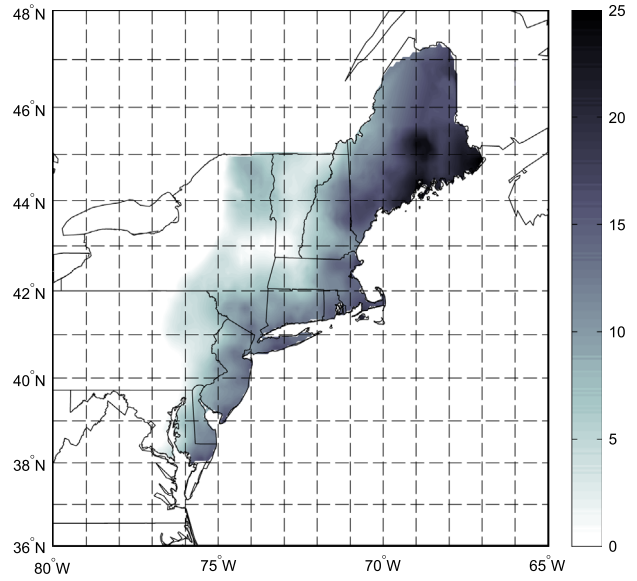

Fig. 9. Expected change (%) in design wind speeds between the 2012 climate scenario and the 2100 climate scenario for ASCE 7–10 Design Category II.

climate scenarios for New York City, was found to be ET-III and can be seen in Fig. 8. As shown in Fig. 8, the 50-year maximum hurricane (only) wind speeds in New York City, under the future climate scenario RCP, are expected to increase for all return periods. For example, the simulated design wind speed associated with ASCE 7–10 (ASCE, 2010) design category II (7% exceedance probability in 50 years, annual exceedance probability=0.00143, MRI=700 years) increases about 14% from the current climate to the future climate. This finding is consistent with the conclusion drawn from the hazard curves (Fig. 7) and suggests that extreme hurricane events in the future (2100) may produce surface wind speeds substantially higher than those produced by extreme hurricanes simulated in the current climate.

The simulated hurricane databases, for the current and future climate scenarios, were then used to create design wind speed maps, comparable to those in ASCE 7–10 (ASCE, 2010). For every zip-code in the study region, design wind speeds were calculated for design categories I, II, and III/IV, as defined in ASCE 7–10 (ASCE, 2010). Fig. 9 shows the difference in wind speeds, between the current climate scenario and the future climate scenario, for ASCE 7–10 (ASCE, 2010) design category II. Design category II wind speeds correspond to a 7% exceedance probability in 50 years (annual exceedance probability=0.00143, MRI=700 years). Based on the simulations performed herein, the majority of the Northeast US coastline is expected to see an increase of about 15% in ASCE 7–10 (ASCE, 2010) design category II wind speeds in the year 2100 compared to the year 2012, with some areas seeing an increase of up to 25%. This is somewhat lower than the increases in design wind speeds obtained in Mudd et al. (2014) which reached nearly 30% in some cases. The less severe increases in design wind speeds obtained in this study are the result of the updated hurricane decay model (Vickery, 2005), which tends to weaken intense hurricanes much more rapidly than the decay model (Vickery and Twisdale, 1995) used in Mudd et al. (2014). In addition, larger increases in design wind speeds were observed when considering more extreme MRI events. This is in agreement with Fig. 8, where larger increases in design wind speeds were seen for longer return period events effecting New York City.

5. Summary and conclusions

Using state-of-the-art empirical, event-based hurricane models and considering one of the RCP climate change scenarios, an analysis was presented to incorporate the possible future climate change impact on the hurricane wind hazard. The IPCC RCP 8.5 climate change scenario for the year 2100 is considered in this study. The US Northeast coastline is used as the study region, which sees the greatest increase in SST under the RCP 8.5 climate change scenario. In addition to consideration of the influence of changes in SST in the gradient wind field and central pressure models (as in Mudd et al. 2014), this study also considers the influence of changes in SST in the decay model.

A total of 10,000 years of hurricane events, under both the current (2012) and future (2100) climate conditions, were simulated to produce a database of simulated maximum hurricane wind speeds for every zip-code in the study region. The resulting database consists of information such as time of hurricane passage, maximum gradient wind speeds, maximum surface wind speeds, radius to maximum gradient wind speeds, as well as tracking information (latitude, longitude, translational velocity, heading angle) for every storm that made landfall in the study region. Information on V_{max} and R_{max} was extracted from the database to form the joint histogram, from which characteristic hurricanes corresponding to different hazard levels (MRI's) were able to be identified. The 50-year maximum wind speed distribution for NYC was provided for comparison of the current climate scenario to the projected future climate scenario RCP 8.5. A significant increase in hurricane intensity for each hazard level was seen, with the increase being larger for more extreme hazard levels.

In summary, this study presents a framework to investigate the effects of climate change on the hurricane wind hazard. Specifically, the effects of changes in sea surface temperature on the hurricane wind field were investigated. Our analysis indicates under the future climate scenario RCP 8.5 in the year 2100, current design wind speeds would be exceeded more frequently and that larger extreme events should be expected. This suggests the need for an increase in design wind speeds in the future in order to ensure target safety and performance levels. However, as noted throughout the paper, the results herein only consider RCP 8.5 and its effects on the gradient wind field, central pressure, and decay models. In order to more accurately assess the effects of changes in SST on hurricane behavior, the hurricane genesis model (i.e., annual hurricane occurrence rate, genesis location) and the

hurricane tracking model (i.e., translational velocity, heading angle) also need to be adapted to account for possible future changes in SST. This work is on-going by the authors.

Further expansion of this framework is also necessary to assess climate change effects on other hurricane hazards such as storm surge and flooding due to rainfall. An understanding of the relationship between the hurricane wind field model, bathymetry, and wind-wave generation is necessary to better assess storm surge flooding. Similarly, an understanding of the coupled relationship between the hurricane wind field model and a rainfall model is necessary to better assess rain-induced flooding. Accounting for these concomitant hazards will allow for the development of risk-consistent designs considering the entire hurricane hazard (i.e., wind, flood, surge). This work is on-going by the authors.

Acknowledgements

The authors are grateful to Dr. Peter Fox from Rensselaer Polytechnic Institute and Mr. Gary Strand from the National Center for Atmospheric Research (NCAR) for running the RCP climate change scenarios in CESM and providing the SST data for the different scenarios. The authors are also grateful to Dr. Franklin Lombardo from Rensselaer Polytechnic Institute for his valuable input and helpful critique of the wind hazard analyses.

References

ASCE, 1993. Minimum Design Loads for Buildings and Other Structures. ASCE Standard 7-93, American Society of Civil Engineers, Reston, VA.

ASCE, 2010. Minimum Design Loads for Buildings and other Structures. ASCE Standard 7-10, American Society of Civil Engineers, Reston, VA.

Bender, M.A., Knutson, T.A., Tuleya, R.E., Sirutis, J.J., Vecchi, G.A., Garner, S.T., Held, I. A., I.A., 2010. Modeled impact of anthropogenic warming on the frequency of intense Atlantic hurricanes. Science 327 (5964), 454–458.

CESM, 2012. ⟨http://www.cesm.ucar.edu⟩. National Center of Atmospheric Research (NCAR).

Darling, R.W. R, 1991. Estimating probabilities of hurricane wind speeds using a large scale empirical model. J. Clim. 4 (10), 1035–1046.

Emanuel, K.A., 1987. The dependence of hurricane intensity on climate. Nature 326, 483–485.

Emanuel, K.A., 2008. The hurricane-climate connection. Bull. Am. Meteorol. Soc. 89, ES10–ES20.

Georgiou, P.N., 1985. Design wind speeds in tropical cyclone-prone regions. Department of Civil Engineering, University of Western Ontario, Canada (Ph. D. dissertation).

Hagen, A.B., Strahan-Sakoskie, D., Luckett, C., 2012. A reanalysis of the 1944–53 Atlantic hurricane seasons—the first decade of aircraft reconnaissance. J. Clim. 25, 4441–4460.

Holland, G.J., Webster, P.J., 2007. Heightened tropical cyclone activity in the North Atlantic: natural variability or climate trend? Phil. Trans. R. Soc. A 365, 2695–2716.

HURDAT, 2013. Atlantic basin hurricane database. Atlantic Oceanographic and Meteorological Laboratory (AOML). National Oceanic and Atmospheric Administration (NOAA). ⟨http://www.aoml.noaa.gov/hrd/hurdat/Data_Storm.html⟩.

IPCC, 2007. Climate Change 2007: Synthesis Report. Contribution of Working Groups I, II and III to the Fourth Assessment Report of the Intergovernmental Panel on Climate Change (Core Writing Team, Pachauri, R.K and Reisinger, A. (Eds.)). IPCC, Geneva, Switzerland, 104 pp.

Irish, J. L.,2008. Predicting the influence of climate change on hurricane flooding. In: Proceedings31st International Conference on Coastal Engineering. Hamburg, Germany.

Knutson, T.R., Sirutis, J.J., Garner, S.T., Vecchi, G.A., Held, I.M., 2008. Simulated reduction in Atlantic hurricane frequency under twenty-first-century warming conditions. Nat. Geosci. 1.6, 359–364.

Landsea, C.W., Anderson, C., Charles, N., Clark, G., Dunion, J., Frenandez-Partagas, J., Hungerford, P., Neumann, C., Zimmer, M., 2004a. The Atlantic hurricane database re-analysis project: documentation for the 1851–1910 alterations and additions to the HURDAT database. In: Murname, R.J., Liu, K.-B. (Eds.), Hurricanes and Typhoons: Past, Present and Future. Columbia University Press, New York, NY, pp. 177–221.

Landsea, C.W., Franklin, J.L., McAdie, C.J., Beven II, J.L., Gross, J.M., Pasch, R.J., Rappaport, E.N., Dunion, J.P., Dodge, P.P., 2004b. A re-analysis of Hurricane Andrew's (1992) intensity. Bull. Am. Meteorol. Soc. 85, 1699–1712.

Landsea, C.W., Glenn, D.A., Bredemeyer, W., Chenoweth, M., Ellis, R., Gamache, J., Hufstetler, L., Mock, C., Perez, R., Prieto, R., Sanchez-Sesma, J., Thomas, D., Woolcock, L., 2008. A reanalysis of the 1911–20 Atlantic hurricane database. J. Clim. 21, 2138–2168.

Landsea, C.W., Vecchi, G.A., Bengtsson, L., Knutson, T.R., 2010. Impact of duration thresholds on Atlantic tropical cyclone counts. J. Clim. 23, 2508–2519.

Landsea, C.W., Feuer, S., Hagen, A., Glenn, D.A., Sims, J., Perez, R., Chenoweth, M., Anderson, N., 2012. A reanalysis of the 1921–1930 Atlantic hurricane database. J. Clim. 25, 865–885.

Lee, K.H., Rosowsky, D.V., 2007. Synthetic hurricane wind speed records: development of a database for hazard analysis and risk studies. Nat. Hazards Rev. ASCE 8 (2), 23–34.

Lin, N., Emanuel, K.A., Oppenheimer, M., Vanmarcke, E., 2012. Physically based assessment of hurricane surge threat under climate change. Nat. Clim. Change 2 (6), 462–467. http://dx.doi.org/10.1038/NCLIMATE1389.

Mann, M.E., Emanuel, K., 2006. Atlantic hurricane trends linked to climate change. EOS 87, 233–241.

Mann, M.E., Sabbatelli, T.A., Neu, U., 2007. Evidence for a modest undercount bias in early historical Atlantic tropical cyclone counts. Geophys. Res. Lett. 34, L22707.

Mudd, L., Y. Wang, C., Letchford, D.V., Rosowsky, 2014. Assessing climate change impact on the us east coast hurricane hazard: temperature, frequency, track. Natural Hazards Review. 10.1061/(ASCE)NH.1527-6996.0000128, 04014001.

Nishijima, K, Maruyama, T., Graf, M., 2012. A preliminary impact assessment of typhoon wind risk of residential buildings in Japan under future climate change. Hydrol. Res. Lett. 6, 23–28.

Powell, M.D., 1990. Boundary layer structure and dynamics in outer hurricane rainbands. Part II: Downdraft modification and mixed layer recovery. Mon. Weather Rev. 118, 918–938.

Rosenthal, T., Hedde, C., Rauch, E., Harwig, R., 2013. 2012 natural catastrophe year in review (Webinar). Retrieved from: ⟨http://www.iii.org/assets/docs/pdf/MunichRe-010313.pdf⟩.

Rosowsky, D.V., Sparks, P.R., Huang, Z., 1999. Wind field modeling and hurricane hazard analysis. Report to the South Carolina Sea Grant Consortium. Department of Civil Engineering, Clemson University, SC.

Sparks, P.R., Huang, Z., 1999. Wind speed characteristics in tropical cyclones. In: Proceedings of the 10th International Conference on Wind Engineering. Copenhagen, Denmark.

Vecchi, G.A., Knutson, T.R., 2008. On estimates of historical north Atlantic tropical cyclone activity. J. Clim. 21 (4), 3580–3600.

Vickery, P.J., Twisdale, L.A., 1995. Wind-field and filling models for hurricane wind-speed prediction. J. Struct. Eng. ASCE, 121; (1700-1209).

Vickery, P.J., Skerlj, P.R., Steckley, A.C., Twisdale, L.A., 2000a. Hurricane wind field model for use in hurricane simulations. J. Struct. Eng. ASCE, 126; a, pp. 1203–1221.

Vickery, P.J., Skerlj, P.F., Twisdale, L.A., 2000b. Simulation of hurricane risk in the U. S. using empirical track model. J. Struct. Eng. ASCE, 126; b, pp. 1222–1237.

Vickery, P.J., 2005. Simple empirical models for estimating the increase in the central pressure of tropical cyclones after landfall along the coastline of the United States. J. Appl. Meteorol. 44, 1807–1826.

Vickery, P.J., Wadhera, D., 2008. Statistical models of Holland pressure profile parameter and radius to maximum winds of hurricanes from flight level pressure and H*Wind data. J. Appl. Meteorol. 44, 1807–1826.

Vickery, P.J., Wadhera, D., Twisdale, L.A., Lavelle, F.M., 2009. United States hurricane wind speed risk and uncertainty. J. Struct. Eng. 135, 301–320.

Wang, Y., 2010. Studies on hazard characterization for performance-based structural design. Department of Civil Engineering, Texas A&M University, USA (Ph. D. dissertation).

Wang, Y., Rosowsky, D.V., 2012. Joint distribution model for prediction of hurricane wind speed and size. Struct. Saf. 35, 40–51.